Sixth International Symposium on Turbulence and Shear Flow Phenomena
Seoul, Korea, 22-24 June 2009

STUDYING TURBULENT MIXED CONVECTION: AN APPROACH BASED ON DIRECT NUMERICAL SIMULATION (DNS) AND SECOND LAW ANALYSIS (SLA)

Petar Kiš
Institute of Thermo-Fluid Dynamics,
Hamburg University of Technology
Denickestr. 17, 21073 Hamburg, Germany
petar.kis@tuhh.de

Heinz Herwig
Institute of Thermo-Fluid Dynamics
Hamburg University of Technology
Denickestr. 17, 21073 Hamburg, Germany
h.herwig@tuhh.de

ABSTRACT

A parallelized code based on spectral methods was developed for future investigations of mixed convection in a turbulent plane channel flow using direct numerical simulations (DNS). The accuracy of the code is demonstrated by very good agreement of our data with those from literature for both the Poisseuille and the buoyancy driven vertical channel flow as an example for the two extremes of forced and natural convection.

Also, some shortcomings of often used reference data for natural convection are pointed out which will help to develop modifications for turbulence models or wall functions especially suited for natural convection.

In order to assess combined momentum and heat transfer problems, the concept of second law analysis (SLA) is introduced from which entropy production rates both due to dissipation and heat transfer can be deduced.

As a first step we illustrate how the friction factor for pure forced convection can be deduced from our DNS data based on the entropy production rate due to dissipation. Consistincy is demonstrated by comparing these results to those based on the wall shear stress.

INTRODUCTION

Turbulent plane channel flow is probably one of the most frequently investigated benchmark cases in computational fluid dynamics since the wall-normal behavior of the flow can easily be investigated without considering edge effects in the streamwise and spanwise directions. For this geometry many researchers have focused on forced convection (e.g. Moser et al., 1999; Jiminez et al., 1991) and some on natural convection (e.g. Boudjemadi et al., 1997; Versteegh and Nieuwstadt, 1999) but only a few were interested in mixed convection yet (e.g. Kasagi and Nishimura, 1997; Iida et al. 2002), although in engineering applications buoyancy effects are almost always superimposed with other driving forces, like moving walls or applied pressure gradients.

In a plane channel mixed convection can be realized in numerous ways and the underlying physics differ just as much. Starting from walls at constant but different temperatures, the *horizontal* channel flow is stratisfied either stably (Iida et al., 2002) or unstably (Iida and Kasagi, 1997), depending on the location of the hot wall. For the *vertical* setup with an upward mainstream direction the buoyancy force stabilizes the aiding flow near the hot wall and destabilizes the opposing flow near the cold wall (Kasagi and Nishimura, 1997). Any tilt between these extremes is conceivable as well, hence, both effects will be blended.

In this paper the vertical channel is analyzed in detail. Driving forces are due to buoyancy and a pressure gradient applied in streamwise direction.

Often the final goal of an analysis of a turbulent shear flow using DNS is providing data for the mean flow values and the correlation terms which appear in the turbulent transport equations. With this knowledge, turbulence models can be adjusted and wall functions can be deduced for RANS simulations.

Here, as an approach to a unifying theory of mixed convection, we also provide the local entropy production rates for a better understanding of the underlying physics. Entropy is produced in two different ways, due to dissipation ($\dot{S}'''_D$) and due to heat conduction ($\dot{S}'''_C$) both occurring at a certain temperature level inside the domain.

Dissipation acts as a source term in the thermal energy balance equation, which, however, is often neglected in DNS. The time average of this quantity slightly differs from the well known pseudo-dissipation ε, which is modelled for RANS computations in an k,ε-model, for example. Only in the limit of infinite Reynolds numbers both dissipation and pseudo-dissipation are equal (Herwig and Kock, 2007). Determination of the dissipation rate directly from DNS data therefore is an attractive alternative and helps to assess the uncertainty involved in the conventional RANS results.

Therefore, the computed data of the present DNS-code may contribute to:

- modelling of near wall turbulent flows
- understanding of the physics utilizing the concept of entropy production

Both aspects will be illustrated after the numerical method is introduced.

NUMERICAL METHOD

The nondimensionalized incompressible Navier-Stokes-equations incorporating the Boussinesq approximation are

integrated in velocity-pressure formulation using a third order semi-implicit Adams-Bashforth/Backward Differentiation scheme (ABBDI3).

$$\frac{\partial u_i}{\partial x_i} = 0 \quad (1)$$

$$\frac{\partial u_j}{\partial t} + \frac{\partial (u_j u_i)}{\partial x_i} + \frac{\partial p}{\partial x_j} = K_u \frac{\partial^2 u_j}{\partial x_i^2} + K_g \theta g_j \quad (2)$$

$$\frac{\partial \theta}{\partial t} + \frac{\partial (\theta u_i)}{\partial x_i} = K_\theta \frac{\partial^2 \theta}{\partial x_i^2} \quad (3)$$

Eq.(3) shows that viscous heating is neglected in the thermal energy balance, nevertheless the entropy production rate is evaluated after every outer time step. Viscous heating will, however, be incorporated into the governing equations in future versions of the code, see Eq.(6) below.

The spatial discretization is based on a pseudo-spectral Chebychev-tau method with periodic boundary conditions using Fourier series both in the streamwise (x) and spanwise (z) directions. The nonlinear terms are treated implicitly in a vorticity-velocity representation while aliasing is prevented by applying the 3/2 rule in every direction. The pressure field is solved directly utilizing the influence-matrix following Kleiser & Schumann (1980) and the tau error arising from the no-slip condition at the walls is corrected. The mean pressure is adjusted dynamically to maintain a constant mass flux, which is zero for pure natural convection and nonzero for forced convection.

The code was written in C++ and parallelized with OpenMP, with the FFTW3 library utilized for the spectral transformations.

All calculations of this study were performed on a Linux-Cluster with 8-16 AMD Opteron-Cores (2.3GHz) per node at a parallel efficiency of 99.4% and above. Typical CPU-times varied between 3-7 weeks with a typical required storage between 6-26GB RAM for each test case.

CONTRIBUTION TO MODELLING

We finally want to contribute to the modelling of turbulent mixed convection. If we want to do so by help of our DNS data we first should demonstrate that they are reliable for the two limiting cases of both natural and forced convection. First, in a comparison with DNS-data from Versteegh and Nieuwstadt (1999) for the natural convection in a vertical channel we show the quality of the present DNS-data. Afterwards, some sample results are presented for forced convection.

Natural convection

Tab.1 contains our results for the four different cases of the study by Versteegh and Nieuwstadt (1999). Results for the Reynolds number based on the friction velocity, Re_τ, the Nusselt number Nu and their relative errors compared to the corresponding results of Versteegh and Nieuwstadt are shown. Also shown are the scaled step sizes Δx^+ and Δy_w^+ (wall nearest Δy^+). All simulations were performed in a domain of size $L_x = 2L_z = 24\delta$, with δ as the channel half width. The grid resolution is fixed at $384 \times 65 \times 192$ in the x, y and z direction, respectively. The resolution as well as the domain size and the Grashof numbers of all four cases are very similar to those of the DNS of Versteegh and Nieuwstadt, hence, direct comparison can be made.

In addition to scalar values like those presented in Tab.1, one of the most important results from DNS are the various terms of the transport equation of the time averaged

Table 1: Four DNS cases for natural convection; comparison with the data of Versteegh and Nieuwstadt (1999) in terms of $\Delta_{\mathrm{Re}_\tau}$ and Δ_{Nu}

Gr	Re_τ	$\Delta_{\mathrm{Re}_\tau}$	Nu	Δ_{Nu}	Δx^+	Δy_w^+
9.5×10^4	61.1	-0.4%	5.37	0.4%	3.82	0.07
15.0×10^4	72.6	2.4%	6.21	0.8%	4.54	0.09
35.2×10^4	100.3	1.2%	8.15	-0.5%	6.27	0.12
88.0×10^4	142.2	0.8%	10.87	-0.3%	8.89	0.17

turbulent kinetic energy $\overline{k}$, which is modelled in every two-equation turbulence model approach. In a vertical plane channel flow this transport equation is:

$$\frac{\partial \overline{k}}{\partial t} = -\overline{u'v'}\frac{\partial \overline{u}}{\partial y} + K_g \overline{u'\theta'} g_x - \frac{\partial \overline{v'k}}{\partial y} + K_u \frac{\partial^2 \overline{k}}{\partial y^2} - \frac{\partial}{\partial y}\overline{v'q'} - K_u \left[\overline{\left(\frac{\partial u'}{\partial x_i}\right)^2} + \overline{\left(\frac{\partial v'}{\partial x_i}\right)^2} + \overline{\left(\frac{\partial w'}{\partial x_i}\right)^2} \right] \quad (4)$$

In Fig.1 each term is illustrated as a function of the wall normal coordinate y for $\mathrm{Gr} = 9.5 \times 10^4$ and compared to the data set of Versteegh and Nieuwstadt. Especially the graphs for shear production and convection of $\overline{k}$ by Versteegh and Nieuwstadt show some unnatural oscillations while the present data are very smooth.

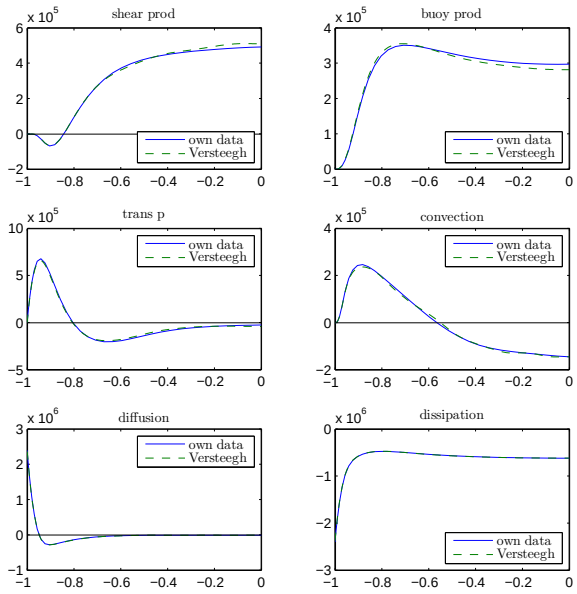

Figure 1: Comparison of the various terms in the transport equation of $\overline{k}$ with the data of Versteegh and Nieuwstadt (1999); full line: own data

As a cross-check for the correctness of the DNS data, the right hand side of Eq.(4) must be zero in a quasi-steady turbulent flow. Fig.2 demonstrates the accuracy of the present data with an error for $\partial \overline{k}/\partial t = 0$ which is three orders of magnitude below the magnitude of the individual terms of the $\overline{k}$-equation. In contrast, the corresponding error of the reference data (Versteegh and Nieuwstadt, 1999) is more than one order of magnitude higher, which is already close to the magnitude of the contributing terms themselve. Since the data of Versteegh and Nieuwstadt represent only one side of the channel, the error in Fig.2 was mirrored at the axis of the channel.

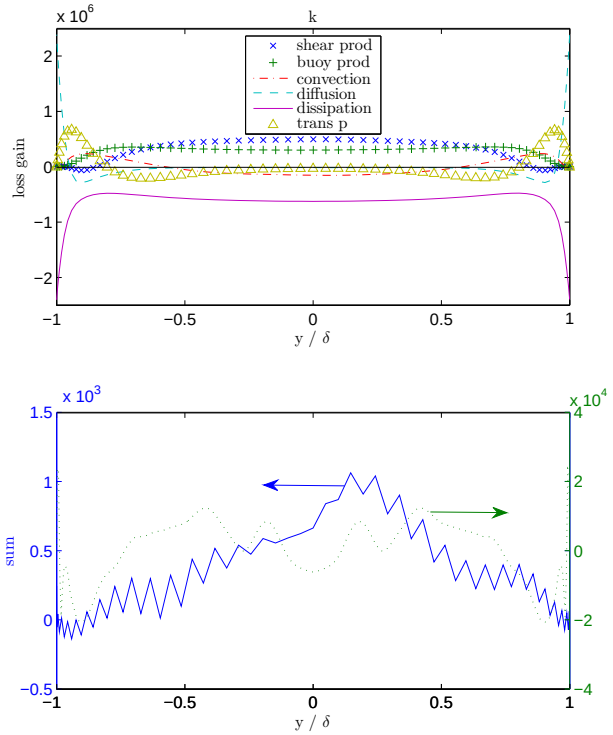

Figure 2: Statistical error of the $\overline{k}$-equation (lower figure) in comparsion with the contributing terms (upper figure); full line: own data, broken line: Versteegh and Nieuwstadt (1999)

Table 2: Sample parameters and results for forced convection

Re_{Dh}	Re_τ	Nu	$N_x \times N_y \times N_z$	Δx^+	Δy_w^+
32000	448.16	13.88	$192 \times 131 \times 192$	14.67	0.13
37333	512.62	15.60	$224 \times 145 \times 224$	14.38	0.12
42667	575.46	17.19	$256 \times 163 \times 256$	14.12	0.11

Forced convection

In pure forced convection the temperature field does not affect the velocity field which means that K_g in Eq.(2) is essentially zero. However, heat transfer with temperature as a passive scalar can be computed simultaneously and a Nusselt number can be deduced. With our own DNS code three heat transfer situations with increasing Reynolds numbers according to Tab.2 have been calculated. For these Reynolds numbers the domain size was chosen to be $L_x = 2L_z = 2\pi\delta$ following Moser et. al (1999). Tab.2 shows the main results in terms of Re_τ and Nu as well as the resolutions in terms of Δx^+ and Δy_w^+.

The results for Re_τ, the mean flow values and the Reynolds stress terms in the transport equations show very good agreement with the data of Moser et al. (1999), although our resolution is not as high as that in their study. With Re_{Dh} and Re_τ according to Tab.2 we also know the friction factor λ_f since

$$\lambda_{f,w} = \frac{8\tau_w}{\rho u_m^2} = 128 \left(\frac{\mathrm{Re}_\tau}{\mathrm{Re}_{Dh}} \right)^2 \qquad (5)$$

Here, the index w indicates that the friction factor is computed via the wall shear stress. A double logarithmic plot of λ_f over Re_{Dh} corresponds to the line for a hydraulically smooth wall in the famous Moody-chart.

The results are shown in Fig.3 and compared to the DNS data of Moser et al. (1999), of the KAWAMURALAB and the THTLAB. Experimental results are approximated by the solid line representing the Dean-correlation (Dean, 1978). The Colebrooke formular for pipe flows (Colebrooke, 1939) which according to the hydraulic diameter concept can be included here, is shown as a dotted line. In the laminar regime the friction factor is $\lambda_f = 96/\mathrm{Re}_{Dh}$ with three numerical results (own data) exactly on this line.

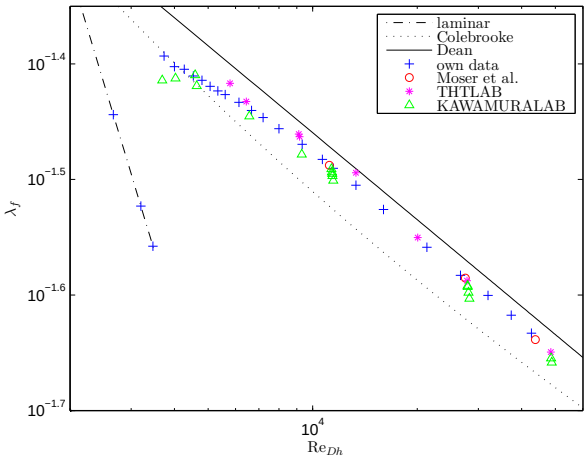

Figure 3: Comparison of the friction factor λ_f for forced convection with other DNS data in a "Moody chart"

For higher Reynolds numbers the friction factors of the present data correspond very well to those of Moser et al. (1999) and the THTLAB, which both were also gained by spectral methods. The data of the KAWAMURALAB from a finite volume method are shown for several domain sizes and resolutions at certain values of Re_τ. A closer look to these data reveals that λ_f has the tendency to grow, if the domain is enlarged or the resolution is increased. In our data, however, λ_f becomes slightly smaller if the resolution is increased.

The slope of the Dean-correlation is very well captured for $\mathrm{Re}_{Dh} > 10^4$. For smaller Reynolds numbers the curve approaches Colebrooke's formular. This tendency is also shown by the data of KAWAMURALAB, although with some higher scatter. The data from THTLAB for Reynolds numbers Re_{Dh} below 2×10^4 have no clear tendency and show some scatter at moderate Reynolds numbers, where the influence of relaminarization effects should still be negligible, however.

For the present DNS the domain size in this moderate Reynolds number regime was enlarged to $2L_x = 5Lz = 10\pi\delta$ while keeping the resolution much higher than needed at $192 \times 131 \times 192$. Despite the bigger domain size and the high resolution it was difficult to achieve convergence for the friction factor. In fact, shear stresses can be evaluated on both walls in a plane channel flow and hence, two friction factors exist. However, in a quasi-steady turbulent flow both should be the same if the time averaging period is long enough. For the Reynolds number $\mathrm{Re}_{Dh} = 32000$ the difference was less than 0.32% of the mean value but for low Reynolds numbers the difference grew to more than 1.5% at $\mathrm{Re}_{Dh} = 4000$. This indicates that for a staedy state analysis of mixed convection Re_{Dh} should be above 10^4 in order to

avoid low Reynolds number effects and long time integration for steady state profiles.

Furthermore, Moser et al. (1999) analyzed the behavior of the mean velocity profile $u^+(y^+)$ and stated that a shear flow would not incorporate low-Renolds number effects for Re_τ higher than 395. This is confirmed with the present DNS data where only the highest three simulations reveal a universal velocity profile.

A similar analysis is suggested for the case of natural convection before it is extended to mixed convection.

CONTRIBUTION TO PHYSICAL UNDERSTANDING

During the postprocessing of a DNS the auto-correlation functions $R_{ii}(x) = \overline{u_i(x_0)u_i(x_0+x)}$ and its spectral transforms, the energy spectra, can be analyzed. As a criterion that the resolution is high enough, the range of the energy spectra should extend at least three orders of magnitude, thus capturing the cascade process of turbulent kinetic energy.

Dissipation in this context more or less is only a vague concept which illustrates the transfer of kinetic energy to the smaller turbulent scales where it finally dissapears. What exactly is dissipation in mathematical terms?

In turbulence models of RANS simulations the term $-\overline{\left(\partial u_j'/\partial x_i\right)^2}$ is referred to as the *dissipation* of turbulent kinetic energy. Since this term is always negative it acts as a sink in the transport equation of $\overline{k}$. A common (mis)conception would consequently be to add the dissipation due to the mean velocity field to this dissipation of turbulent kinetic energy in order to achieve the over all dissipation rate. This, however, is only the so-called *pseudo-dissipation*.

Instead, the real dissipation appearing as a source in the thermal energy balance and hence, transforming kinetic into thermal energy is slightly different. If the dissipation is taken into account correctly then Eq.(3) must be modified.

With dissipation included as a source of thermal energy, a sink due to buoyant acceleration of the flow must be considered as well, in order to fullfill the overall energy balance. Since for pure natural convection, for example, no net heat is produced inside the channel, the heat fluxes through both walls then have to be the same. The extended thermal energy equation including all these effects now reads (c.f. Eq.(3))

$$\frac{\partial\theta}{\partial t} + \frac{\partial\left(u_i\theta\right)}{\partial x_i} = K_\theta \frac{\partial^2\theta}{\partial x_i^2} - \mathrm{Ec}K_g\theta u_j g_j + \mathrm{Ec}K_u \frac{1}{2}\left(\frac{\partial u_j}{\partial x_i} + \frac{\partial u_i}{\partial x_j}\right)^2 \quad (6)$$

A more general concept to account for irreversible processes based on a second law analysis (SLA) should link the dissipation to the entropy production in the flow field. Dissipation in Eq.(6) basically is the term $\dot{S}'''_D$ which contributes to a nondimensionalized entropy production rate:

$$\dot{S}''' = \underbrace{\frac{1}{2}\left(\frac{\partial u_j}{\partial x_i} + \frac{\partial u_i}{\partial x_j}\right)^2}_{\dot{S}'''_D} + \underbrace{\frac{\varepsilon}{\mathrm{Ec}\,\mathrm{Pr}}\left(\frac{\partial\theta}{\partial x_i}\right)^2}_{\dot{S}'''_C} \quad (7)$$

The local entropy production rate can be integrated over the whole domain to compute the overall entropy production rate.

$$\dot{S} = \int_V \dot{S}'''\, dV \quad (8)$$

If the entropy production is evaluated for RANS computations it must be splitted into a mean and a turbulent part, for details see Herwig and Kock (2007).

$$\dot{S}'''_{D,C} = \dot{S}'''_{\overline{D},\overline{C}} + \dot{S}'''_{D',C'} \quad (9)$$

Fig.4 illustrates the time averaged and nondimensionalized mean and turbulent parts of the entropy production rates across the channel for forced convection at $\mathrm{Re}_{Dh} = 32000$.

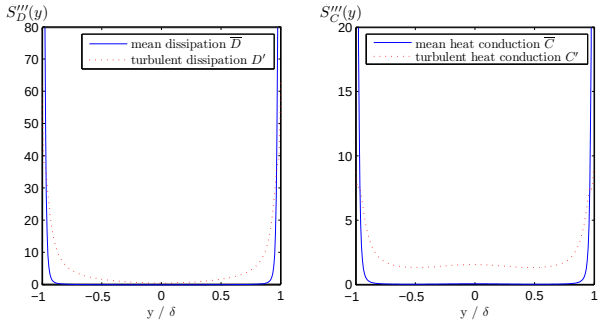

Figure 4: Time and spatial averaged (x and z directions) entropy production rate due to dissipation $\dot{S}'''_D$ and heat conduction $\dot{S}'''_C$ splitted into a mean and a turbulent part at $\mathrm{Re}_{Dh} = 32000$

As expected the entropy production due to the mean values has its peaks at the walls where the mean gradients are steepest. Also, the maxima of the entropy production due to turbulent dissipation $\dot{S}'''_{D'}$ is located at the walls, although not as high as its mean counterparts. In the middle of the channel both contributions to entropy production due to dissiaption have a local minimum. This is different for the entropy production due to heat conduction since $\dot{S}'''_{C'}$ takes a local maximum on a fairly low level. In contrast to the entropy production due to dissipation this local maximum is much higher than its mean counterpart $\dot{S}'''_{\overline{C}}$.

According to Eq.(7) the graphs of dissipation and conduction cannot be compared directly as it remains to choose $\varepsilon = \Delta T/T$ and the Eckert number $\mathrm{Ec} = u_{ref}^2/(c_p\Delta T)$ as well as the Prandtl number Pr. In fact, one key aspect of entropy production is the temperature level apearing in ε at which thermal energy is produced and conducted.

Now, the integrated local entropy production due to dissipation $\dot{S}'''_D$ is directly linked to the kinetic energy losses of the flow, i.e. the total pressure drop, as it represents the transformation of kinetic into inner energy. Hence, after some mathematical manipulations the friction factor based on entropy production follows (c.f. Herwig et al., 2008).

$$\lambda_{f,s} = \frac{16}{\mathrm{Re}_{Dh}}\frac{\partial}{\partial x}\left(\dot{S}_{\overline{D}} + \dot{S}_{D'}\right) \quad (10)$$

$$= \frac{16}{\mathrm{Re}_{Dh}}\int_{-1}^{1}\int_0^{L_z}\left(\dot{S}'''_{\overline{D}} + \dot{S}'''_{D'}\right)\, dz\, dy \quad (11)$$

After inserting Eq.(8) into Eq.(10) it turns out that differentiation and integration with respect to x cancel.

With Eq.(11) the friction factor $\lambda_{f,s}$ can be computed by integration over the time averaged local dissipation rate. These results can be compared to the friction factors $\lambda_{f,w}$ of the three highest Reynolds numbers from the previous section, see Tab.3.

The small relative error demonstrates the good agreement with the standard procedure of evaluating the wall

Table 3: Comparison of the computed friction factors based on the wall shear stress ($\lambda_{f,w}$) and the local entropy production due to dissipation ($\lambda_{f,s}$)

Re_{Dh}	$\lambda_{f,w}$	$\lambda_{f,s}$	rel. error
32000	0.02511	0.02466	1.8 %
37333	0.02413	0.02372	1.7 %
42667	0.02328	0.02292	1.5 %

shear stress. It is interesting to see how the error in Tab.3 decreases while the Reynolds number increases. This is due to the fact that for the higher Reynolds numbers the flow domain was slightly better resolved as it follows from Δx^+ and $\Delta y{+}_w$ in Tab.2. Thus, a better resolution of the smallest turbulence scales is achieved such that their contribution to the dissipation can be considered. At $\mathrm{Re}_{Dh} = 10667$, for example, the relative error is only 0.08%, since the flow field resolution is almost twice as good as for the highest Reynolds number in Tab.2 and 3. For $\mathrm{Re}_{Dh} = 10667$ step sizes are $\Delta x^+ = 8.40$ and $\Delta y_w^+ = 0.05$.

This behavior also explains, why the friction factor $\lambda_{f,s}$ is always smaller than $\lambda_{f,w}$ when the resolution is not high enough to capture the smallest scales. This in turn can be used as a benchmark cross check for a proper resolution.

For the assessment of the two contributing parts, mean and turbulent dissipation, it is noted that both integral values are of the same order of magnitude and for $\mathrm{Re}_{Dh} = 42667$ are almost identical.

A time and/or spatially averaged entropy production rate does not reveal anything about the time depending physics. Therefore, the following two maps illustrate the two-dimensional distribution (in a x, y-plane) of both, the entropy generation due to dissipation and heat conduction at a certain time step of forced convection at $\mathrm{Re}_{Dh} = 32000$. Regions of low entropy production are blue and those of high entropy production are red. In streamwise direction only half of the solution domain is shown.

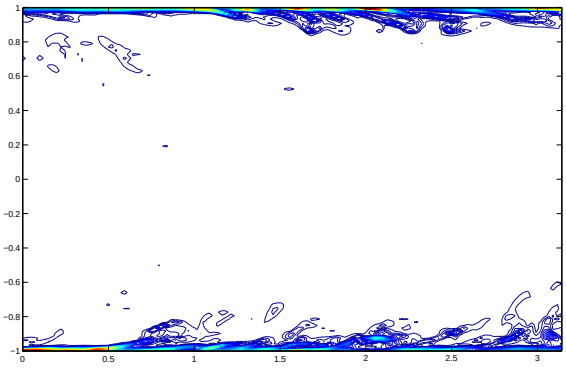

Figure 5: Entropy production due to dissipation at a certain time step for forced convection at $\mathrm{Re}_{Dh} = 32000$

Both figures reveal the well known wall bounded elongated structures of a turbulent shear flow. For entropy production due to heat transfer those structures appear even in the center of the channel. The structures close to the wall for the entropy production due to dissipation and heat conduction show some similarity which demostrates the connection of the two contributing mechanisms. This is due to the fact that steep temperature gradients an hence high entropy production due to heat conduction occur where fluid

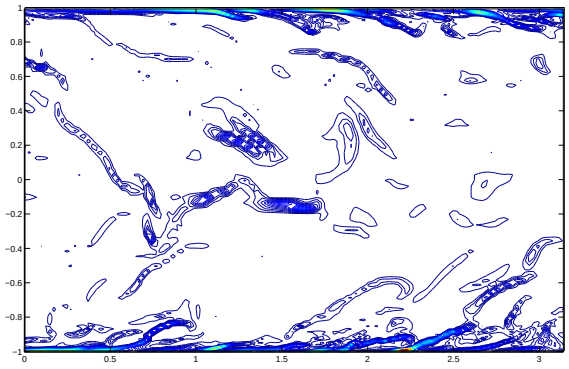

Figure 6: Entropy production due to heat conduction at a certain time step for forced convection at $\mathrm{Re}_{Dh} = 32000$

is strongly convected to a region of different temperature.

The regions of high dissipation are very small and wall bounded but do not show a streamwise connection. Instead, even close to the wall regions of high dissipation coexist next to regions of low dissipation. The same applies to the entropy production due to heat conduction, however, with lower extreme values as Fig.4 has already shown.

In order to convey a better three dimensional image of the locally distributed entropy production rate, Fig.7 illustrates the distribution of a certain iso-value of the entropy production due to dissipation. Again, only half of the solution domain is shown in streamwise and only a third in spanwise direction.

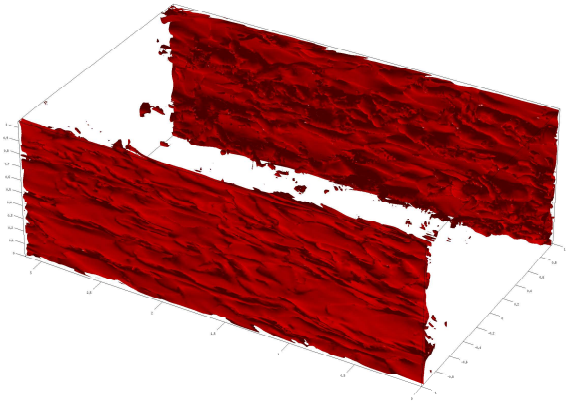

Figure 7: Iso-surface of an arbitrarily chosen isovalue of the entropy production due to dissipation in forced convection at $\mathrm{Re}_{Dh} = 48000$

The iso-surfaces of dissipation are in fact three dimensional structures which follows from the different visable shapes at the two walls. Close to the wall the iso-surfaces seem to be smoother and streamwise orientated. Closer to the center the isosurfaces become rougher and complex in their structure showing much more similarity to the structures already identified in Fig.5 and Fig.6.

The structures of the local entropy production rate due to dissipation in Fig.7 are related to the isosurfaces of vorticity, not only mathematically but also visually as Fig.8 demonstrates.

Correspondance is cleary seen, especially for the isosurface facing the wall. Although, the structures seem more tube-like, bigger and less smooth. However, the two isovalues for entropy production and vorticity were chosen abritraily in order to have visible structures in the same region of the channel. Modifications of the iso-values do change the shape and size of the structures.

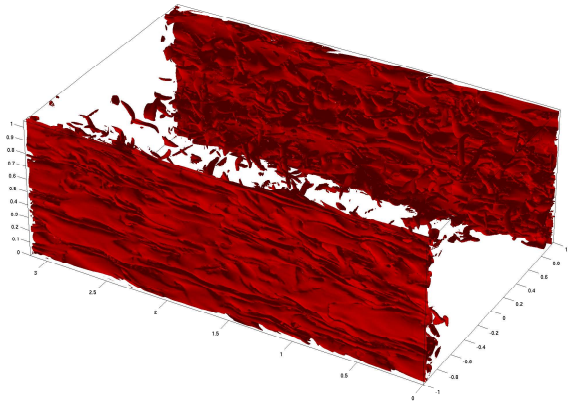

Figure 8: Isosurface of an arbitrarily chosen isovalue of the vorticity $|\nabla \times \mathbf{u}|$ for forced convection at $\mathrm{Re}_{Dh} = 48000$

CONCLUSION AND OUTLOOK

The two limiting cases of mixed convection for the vertical channel with constant but different wall temperatures were examined. It could be shown that the results from our code for both, forced and natural convection agree very well with the DNS data from literature.

Especially our DNS data for natural convection revealed some shortcomings of the reference data and demonstrated the ability to compute the contributing terms of the Reynolds stress budgets with high accuracy.

In the case of forced convection the friction factor λ_f was used as a comparison parameter. Very good agreement to other DNS data was shown. A clear tendency of our own data for λ_f in the range of low to moderate Reynolds numbers ($\mathrm{Re}_\tau = 66 - 575$) appears, with λ_f on a straight line for $\mathrm{Re} \to \infty$ in the "Moody chart". In order to investigate forced convection without the influence of low-Reynolds number effects, Re_τ should be above 400.

A similar analysis for natural convection must be performed as well, using the Grashof number Gr as the crucial parameter. With parameters above the "critical values" the analysis of mixed convection is expected to be free of low-Reynolds number effects, too, although the stabilizing and destabilizing mechanisms encountered in mixed convection may be responsible for a more complicated behavior of the flow.

The concept of a second law analysis for mixed convection was introduced as a valuable tool for the assessment of convective heat transfer problems. The governing equations were not yet modified although the computed dissipation can be easily carried over as a source term to the thermal energy balance. For the consistency of the overall energy balance it was shown that when buoyancy is involved the production of kinetic energy, which acts as a sink term in the thermal energy balance, must also be incorporated.

As a first example for the significance of the entropy production rate it was shown how the friction factor for forced convection can be deduced from the integrated local entropy production due to dissipation. The results were compared to the traditional way using the wall shear stress and showed good agreement with an error of 1.5% for the highest Reynolds number presented in this paper. The friction factor $\lambda_{f,s}$ was always smaller than $\lambda_{f,w}$ which is due to the still insufficient resolution of the smallest turbulent scales in the present DNS data.

The relation between the dissipation rate and the absolute value of the vorticity was illustrated qualitatively as their mathematical representations already suggest this similarity. Finally, the structures of the entropy production rate due to dissipation and heat conduction were compared. It was shown that in both cases elongated coherent structures exist. The entropy production rate due to heat conduction, however, is not as much concentrated in the near wall region as the entropy production due to dissipation.

With our approach to analyse turbulent mixed convection flows with the tools of DNS and second law analysis (SLA) we hope to further contribute to the modelling and understandingof complex turbulent flows in the near future.

REFERENCES

Boudjemadi, R., Maupu, V., Laurence, D., and Le Quere, P., 1997, "Budgets of Turbulent Stresses and Fluxes in a Vertical Slot Natural Convection at Rayleigh Ra=10^5 and 5.4×10^5", *Int. J. Heat and Fluid Flow*, Vol. 18, pp. 70-79

Canuto, C., Hussaini, M. Y., Quarteroni, A., and Zang, T.A., 1988, "Spectral Methods in Fluid Dynamics", *Springer*

Colebrook, C. F., 1939, "Turbulent flow in pipes with particular reference to the transition between the smooth and rough pipe laws", *J. Inst. Civil Engrs Lond.*, Vol. 11, pp. 133-156

Dean, R. B., 1978, "Reynolds Number Dependencies of Skin Friction and Other Bulk Flow Variables in Two-Dimensional Rectangular Duct Flow", *J. Fluids Engineering*, Vol. 100, pp. 215-223

Herwig, H., and Kock, F., 2007, "Direct and Indirect Methods of Calculating Entropy Generation Rates in Turbulent Convective Heat Transfer Problems", *Int. J. Heat and Mass Transfer*, Vol. 43, pp. 207-215

Herwig, H., Gloss, D., Wenterodt, T., 2008, "A New Approach to Understanding and Modelling the Influence of Wall Roughness on Friction Factors for Pipe and Channel Flows", *J. Fluid Mech.*, Vol. 613, pp. 35-53

Iida, O., Kasagi, N., and Nagano, Y., 2002, "Direct Numerical Simulation of Turbulent Channel Flow Under Stable Density Stratification", *Int. J. Heat and Mass Transfer*, Vol. 45, pp. 1693-1703

Iida, O., and Kasagi, N., 1997, "Direct Numerical Simulation of Unstably Stratisfied Turbulent Channel Flow", *J. Heat Transfer*, Vol. 119, pp. 53-61

Jimenez, J., and Moin, P., 1991, "The minimal flow unit in near-wall turbulence", *J. Fluid Mech.*, Vol. 225, pp. 213-240

Kasagi, N., and Nishimura, M., 1997, "Direct Numerical Simulation of Combined Forced and Natural Turbulent Convection in a Vertical Plane Channel", *Int. J. Heat Fluid Flow*, Vol. 13, pp. 88-99

KAWAMURALAB, data collection see: mura-sun.me.noda.tus.ac.jp/turbulence

Kleiser, L., and Schumann, U., 1980, "Treatment of Incompressibility and Boundary Conditions in 3-D Numerical Spectral Simulations of Plane Channel Flow", *Third GAMM Conference Numerical Methods in Fluid Mechanics*, pp. 165-173

Moser, R. D., Kim, J., and Mansour, N. N., 1999, "Direct Numerical Simulation of Turbulent Channel Flow up to $\mathrm{Re}_\tau = 590$", *J. Fluid Mech.*, Vol. 11, pp. 943-945

Peyret, R., 2002, "Spectral Methods for Incompressible Viscous Flow", *Springer*

THTLAB, data collection see: www.thtlab.t.u-tokyo.ac.jp